AJNR

The Radiographic Characterization of Burst Fractures of the Spine

Scott W. Atlas, Victor Regenbogen, Lee F. Rogers and Kwang S. Kim

The Radiographic Characterization of Burst Fractures of the Spine

Scott W. Atlas[1,2]
Victor Regenbogen
Lee F. Rogers
Kwang S. Kim

A retrospective review of 75 burst fractures of the spine was performed to define the radiographic features found on high-resolution CT, polytomography, and plain radiography and thereby allow full characterization of this uncommon spinal injury. Characteristic components of the injury include: (1) centripetally oriented disruption of the vertebral body, (2) unilateral or bilateral laminar fractures that abut the spinous process, (3) marked anterior wedging, (4) vertically oriented vertebral fracture emanating from the basivertebral foramen, (5) increased interpediculate distance, and (6) significant spinal canal narrowing by characteristic retropulsed fragments. Nearly all bursts occurred from T9 to L5; double bursts were present in less than 10% of cases. The usually present neurologic deficit nearly always corresponded to the level of the burst rather than to the frequently found discontiguous associated spine fracture. Recent literature suggests that these complex fractures, which were initially thought to represent stable injuries, are often unstable. A subcategorization of burst fractures and their variants is proposed to explain this instability. An approach to the radiographic diagnosis of the spinal burst is proposed, and plain film clues to distinguish the burst fracture from the more common compression fracture are discussed. Representative cases are illustrated.

The burst fracture is a specific form of compression fracture of the vertebral body wherein a fragment arising from the posterosuperior margin of the vertebral body is displaced into the spinal canal. The retropulsed fragment may result in neurologic injury to the spinal cord, conus medullaris, or cauda equina. There are specific clues to the presence of this injury on plain radiographs that warrant further evaluation by either polytomography or CT to determine the degree of spinal canal compromise, the presence of associated posterior element fractures, and the nature of the retropulsed fragment. Although initially described as "stable" injuries, recent literature suggests that these complex fractures often behave in an unstable manner [1–8].

We review a series of 75 burst fractures of the spine and define the radiographic features found on high-resolution CT or plain tomography that allow full characterization of this lesion. Plain film clues to distinguish a burst fracture from the more common compression fracture are stressed.

Materials and Methods

Clinical records and radiographs of all patients admitted to Northwestern Memorial Hospital with spine trauma since June 1973 were reviewed retrospectively.

Seventy-five fractures in 69 patients (55 men, 14 women; ages 15–64; mean age 28.7; median age 25) were classified as spinal burst fractures after detailed radiographic analysis. All patients had high-quality plain and/or CT for evaluation of the acute injury. Thirty-two patients sustained their injury from a fall, 23 were involved in auto accidents, six were in motorcycle accidents, and eight were injured in a variety of other situations.
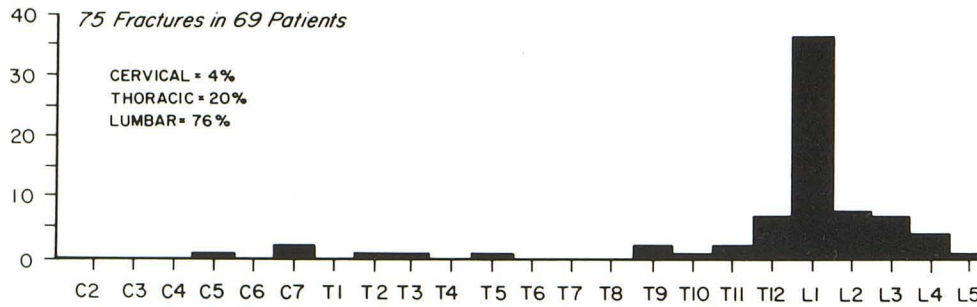
Fig. 1.—Distribution of burst fracture levels.

Results

Distribution of Burst Fractures

The anatomical distribution of burst fracture level is shown in Figure 1. Sixty-nine of 75 burst fractures (92%) occurred from T9 to L5; 37 of 75 bursts (50%) were found at L1, the most common site. Six of 69 patients (8.7%) had burst fractures at two levels: T2–T3 (1), T10–L2 (1), T11–T12 (1), L1–L4 (1), and L1–L2 (2).

Typical Features of the Burst Fracture

Sagittal Vertebral Body Fracture. Sixty-six of 75 burst fractures (88%) had a typical vertically oriented fracture component in the vertebral body, involving the inferior half of the vertebra and extending to the region of the basivertebral foramen.

Posterior Element Involvement. In 11 of 75 bursts (14.7%), no posterior element fracture was identified on tomographic or CT examination. Unilateral posterior element fractures were present in 29 cases (38.7%), while bilateral posterior element fractures were seen in 35 cases (46.6%). Four patients with no sagittal vertebral body component did have posterior element fractures. Seventy percent of laminar fractures were located adjacent to (with or without extension into) the spinous process.

Interpediculate Distance. Interpediculate distances (IPD) were measured in all cases at the level of the burst and compared with the IPD at the level above and below. Although normal IPD ranges have been established [9], there is a variation of IPD in each patient, from level to level. In the three patients with neither vertical vertebral body fracture nor posterior element fracture, no focal increase in IPD exceeded 3 mm at the burst level. Therefore, a focal increase of 4 mm was considered remarkable. Eighty-one percent had focal increase in IPD greater than or equal to 4 mm when compared with the level above or the level below, while 19% had no significant focal increase in IPD at the level of the burst. Sixty-three percent had an increase in IPD greater than or equal to 4 mm compared with *both* the level above *and* below the burst. Twelve percent had an increased IPD compared only with the level below the burst, while 6% had an increased IPD compared only with the level above the burst.

Anterior Wedge Deformity. Anterior wedge deformity of the

TABLE 1: Degree of Anterior Wedging

Grade*	% of Cases
I	24.6
II	53.6
III	21.7
IV	0

* Grade I = 0%–24% loss of height, Grade II = 25%–49% loss of height, Grade III = 50%–74% loss of height, Grade IV = 75%–100% loss of height.

TABLE 2: Degree of Spinal Canal Narrowing

Level	Range (%)	Average (%)
Cervical	20–85	48.3
Thoracic	30–90	59.3
Lumbar	5–90	57.3
All cases	5–90	57.3

TABLE 3: Contiguity of Associated Spinal Fractures with Burst Level*

Distance from Burst		No. of Cases	Percent of Total
(±)	1 level	10	41.7
	2 levels	4	16.7
	3 levels	2	8.3
	>3 levels	8	33.3

* In 24 patients with vertebral body and/or posterior element fractures at a level different from the burst fracture.

involved vertebral body was quantitatively assessed in all patients, comparing vertebral body height with the vertebra above (Table 1). Grades I–IV were assigned with respect to degree of loss of height, so that Grade 1 = 0%–24% decrease, Grade II = 25%–49% decrease, Grade III = 50%–74% decrease, and Grade IV = 75%–100% decrease. Three patients (4.3%) had no measurable loss of height at the anterior margin of the burst vertebral body. The average degree of anterior wedging measured 35.4%.

Spinal Canal Narrowing. Spinal canal narrowing by the retropulsed fragment from the posterosuperior corner of the vertebral body was measured from tomography or CT in all cases at the point of greatest narrowing, in the dimension of greatest narrowing (i.e., anteroposterior or lateral) (Table 2).

Fig. 2.—Patterns of the retropulsed fragment. CT analysis of retropulsed fragment from posterosuperior aspect of vertebral body in 15 cases revealed four basic patterns as shown. Note characteristic laminar fracture adjacent to junction with spinous process (arrow).

NORMAL

SINGLE
7/15 (46.7%)

SAGITTAL SPLIT
3/15 (20%)

ASYMMETRIC SPLIT
3/15 (20%)

UNILATERAL SPLIT
2/15 (13.3%)
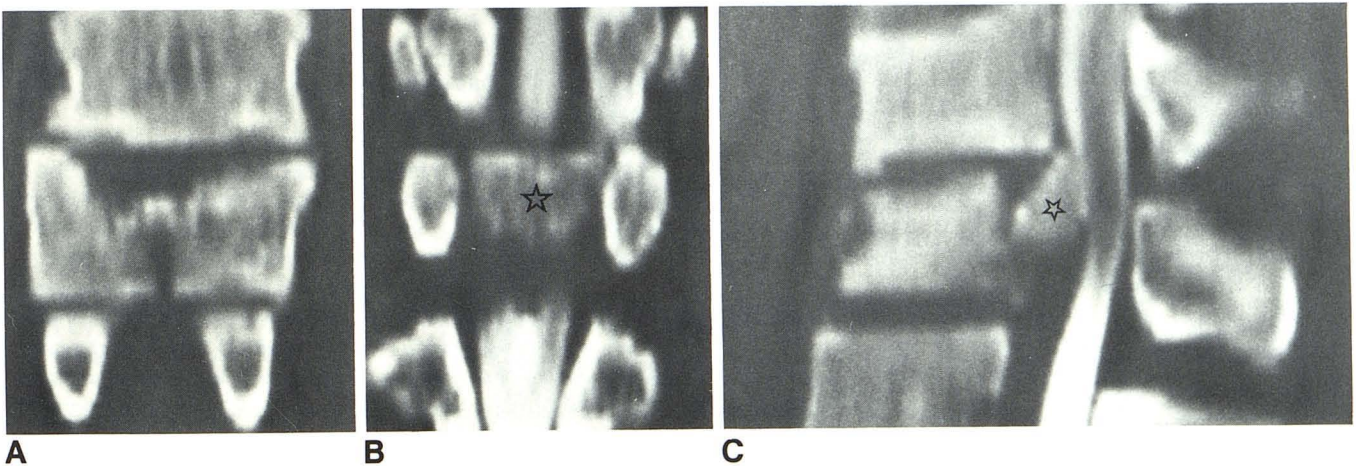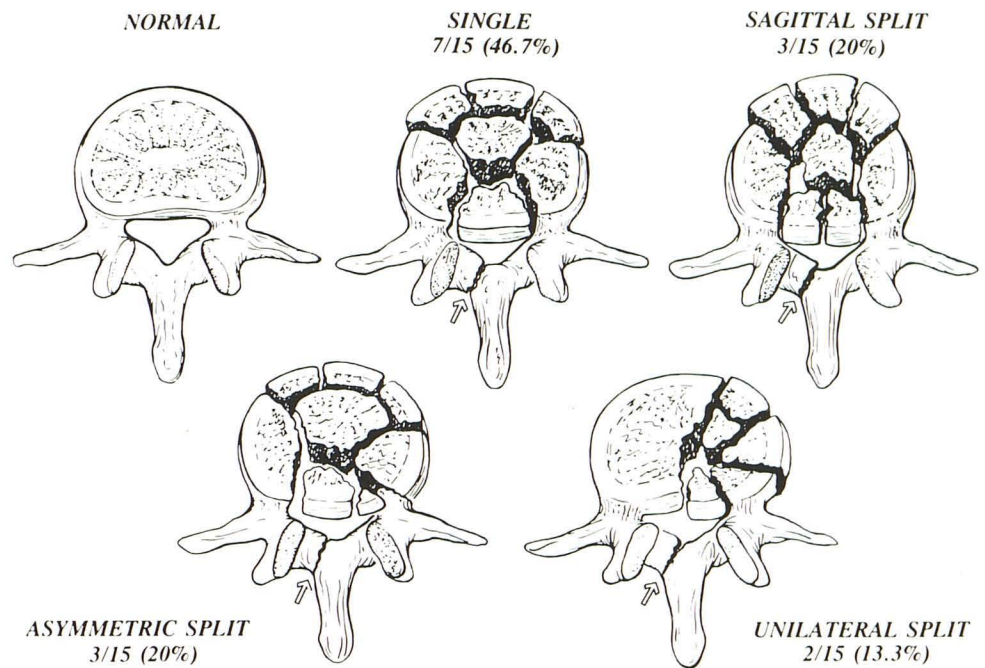

A   B   C

Fig. 3.—The utility of reformatting techniques in fragment characterization. Coronal (A and B) and sagittal (C) reformations from metrizamide CT scan clearly demonstrate location and size of retropulsed fragments (star), components of burst injury, and consequent impingement on spinal cord.

Canal narrowing ranged from 5% to 90%, with average canal compromise measuring 57.3%.

Associated Spinal Fractures

Thirty of 69 patients (43.5%) had associated spine fractures at other levels. In these patients, two had isolated spinous process fractures (6.7%), four had isolated transverse process fractures (13.3%), and 24 had associated vertebral body/posterior element fractures (80%). In these 24 patients, contiguity of the associated fractures with the burst level was tabulated (Table 3). Fourteen of 24 associated fractures (58.3%) were located more than one level from the burst, while eight of these (33.3%) were more than three levels from the burst.

Associated Neurologic Injury

Neurologic sequelae from vertebral burst fractures are common. In our series, 45 of 69 patients (65.2%) presented with acute neurologic deficits.

Of 20 patients with neurologic deficit who had associated vertebral body or posterior element fracture at another level, the neurologic level corresponded with the burst level in 19 cases (95%), rather than with the level of the associated fracture.
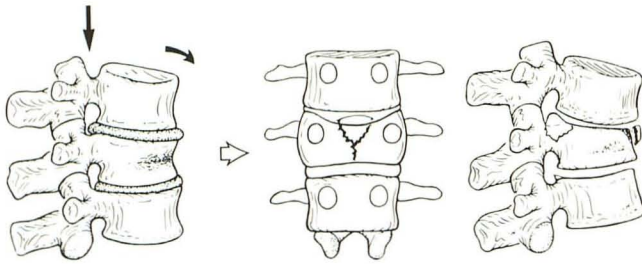
Fig. 4.—Basic mechanism of injury. Dominant axial load (*straight arrow*) with superimposed flexion (*curved arrow*). Note typical appearance of involved body on anteroposterior and lateral views. Characteristic features include: (1) compression of superior (± inferior) endplates, (2) widened interpediculate distance, (3) retropulsed fragment, (4) sagittal split extending to basivertebral foramen, and (5) displaced anterosuperior fragment.

TYPE A (22.7%)   TYPE B (54.7%)   TYPE C (0%)
DUAL RETROPULSION   CLASSIC BURST   POSTEROINFERIOR
                                                RETROPULSION

TYPE D1 (17.3%)   TYPE D2 (2.7%)   TYPE E (2.7%)
BURST-LATERAL   BURST-SAGITTAL   UNILATERAL
TRANSLATION   TRANSLATION   BURST

Fig. 5.—Classification of burst fractures, modified from Denis [11] (*star* = retropulsed fragment).

No definite correlations existed between radiographic appearance and neurologic status. Specifically, posterior element fracture, associated translation, and degree of spinal canal narrowing were not predictive of neurologic deficit.

The Retropulsed Fragment

CT analysis of the retropulsed fragment from the posterosuperior aspect of the vertebral body in 15 cases revealed four basic patterns (Fig. 2). The midline single fragment was seen most commonly (46.7%). Fragment location and characterization were more clearly delineated by CT in the axial plane. Reformatting techniques allowed coronal and sagittal visualization of the fragment, and when combined with low-dose intrathecal metrizamide, provided more information than myelography alone (Fig. 3).

Mechanism of Injury

The basic mechanism of injury in spinal burst fractures has been discussed by many authors [2, 6, 10–12]. Axial compressive forces, with varying degrees of flexion force, result in the characteristic skeletal deformities (Fig. 4). When rotational forces are superimposed upon the dominant axial load, burst variants result.

Classification of Burst Fractures

Spinal burst fractures can be classified according to radiographic appearance (Fig. 5). Dual retropulsion bursts (type A) occurred in 22.7% of our cases. In these fractures, fragments originating from both the posterosuperior and posteroinferior margins of the involved vertebral body are retropulsed into the spinal canal. The classic burst (type B) was most common in our series (54.7% of cases). With retropulsion from the posterosuperior corner, the inferior endplates remain intact. The type C burst, with isolated posteroinferior retropulsion and intact superior endplates, is theoretically
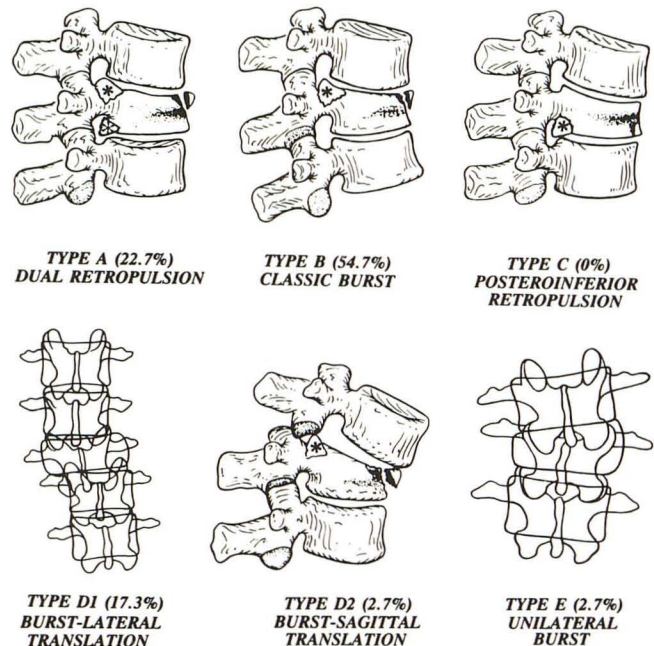
presumed and has been reported [11], although no cases were identified in our series.

Burst translation can be subdivided into two subsets, according to the predominant direction of translation. All type D bursts occurred in single-level bursts. Type D_1, or burst-lateral translation fractures, result from axial compression with a significant component of lateral rotation/flexion. Correct diagnosis is predicated upon obtaining an anteroposterior view, as the lateral view alone may not even suggest this injury. Burst-sagittal translation fractures (type D_2) were rare, occurring in only 2.7% of cases. These complex fracture-dislocations result from axial compression with an accompanying hyperflexion, so that facet perching or frank locking occur. These fractures can be suspected when the kyphotic deformity on the initial lateral view is marked. The unilateral burst (type E) was also infrequent (2.7%). In these unusual fractures, marked comminution involves predominantly one side of the vertebra, so that the retropulsed fragment originates from that side only. An acute lateral flexion, in combination with axial loading, is responsible for this peculiar fracture. CT is superior in identifying this type of burst.

Approach to Radiographic Diagnosis

Several clues on plain radiography suggest the presence of the burst fracture and allow differentiation from the more common, and less worrisome, wedge compression fracture. On presentation to the emergency room, both lateral and anteroposterior radiographs should be obtained. On the *lateral* radiograph, after noting a wedge deformity of the vertebral body, attention should be directed to the posterosuperior

Fig. 6.—Case 1. Classic burst (see text for full description). **A**, Lateral; **B**, Anteroposterior; **C**, Axial CT; **D**, Axial CT.
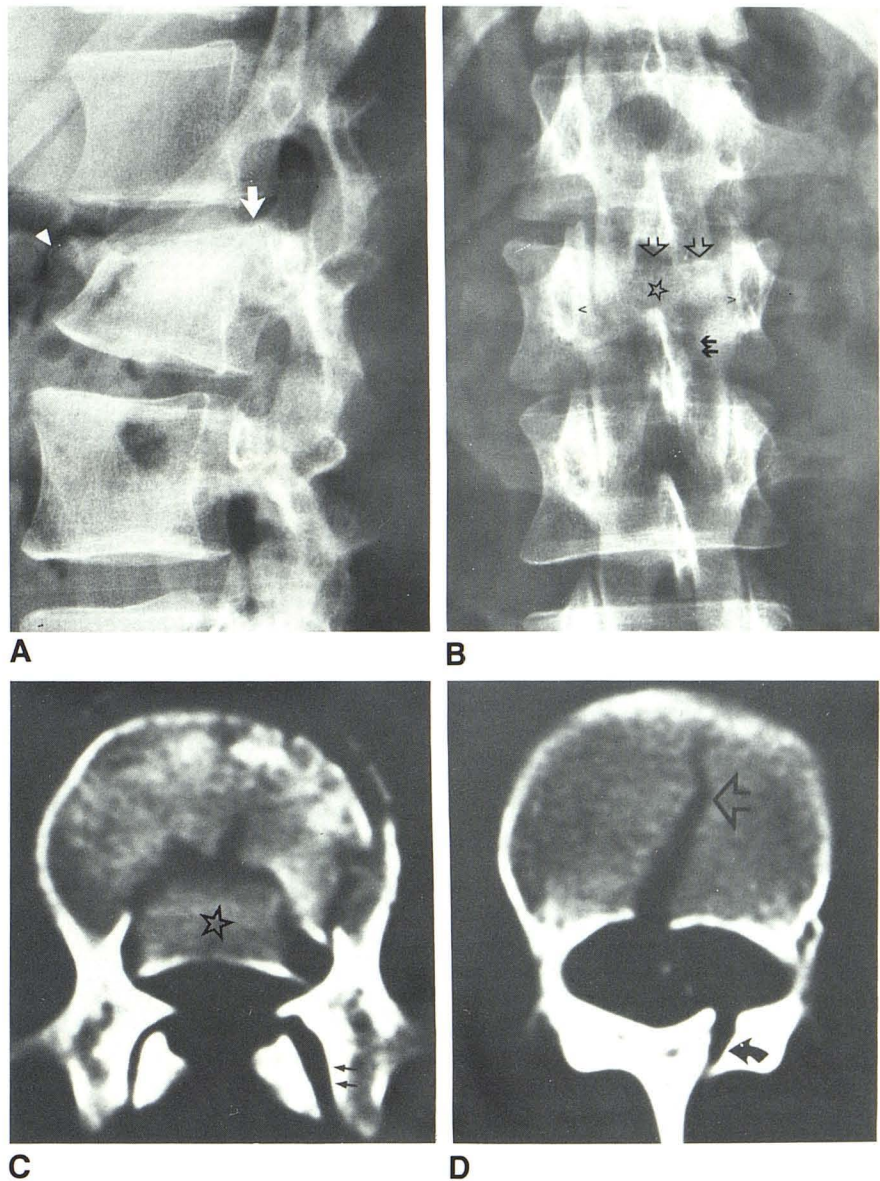
corner of the vertebral bodies to identify a retropulsed fragment. Significant kyphosis at the involved level can signify the presence of a burst-translation, an unstable injury. Facet alignment should be scrutinized. On the *anteroposterior* radiograph, malalignments, such as unsuspected lateral translation, can be missed if one relies solely on the lateral film. A focal increase in interpediculate distance signifies posterior element disruption, another indicator of instability. The margins of the vertebral bodies should be identified, with particular attention to the superior margins, as the retropulsed fragment can be visualized on the anteroposterior view if specifically sought. Vertical fracture components in the vertebral body, pedicle, and lamina can also be identified. The search for specific anatomical derangements, as illustrated by the following cases, will result in the definition of the injury as well as proper triage for further evaluation by CT or tomography.

Approach to Radiographic Diagnosis

Case 1 Classic Burst (see Fig. 6). On the lateral view (Fig. 6A), scrutinize the posterosuperior margin of the vertebral body for the retropulsed fragment (arrow). Note the double density of the cortical bone as a consequence of fragment rotation. Anterior wedge deformity greater than 25%, as in this case, was present in 75.6% of cases. Also note the displaced anterosuperior fragment (arrowhead). On the anteroposterior view (Fig. 6B), widened interpediculate distance (arrowheads), angulation of superior endplates (open arrows) and obscuration of inferior endplates, and left perispinous laminar fracture (small arrows) can be seen. The major retropulsed fragment (star) is also visualized. The sagittal vertebral body fracture is not seen. CT (Figs. 6C and 6D) clearly defines the retropulsed midline fragment (star) and subsequent spinal
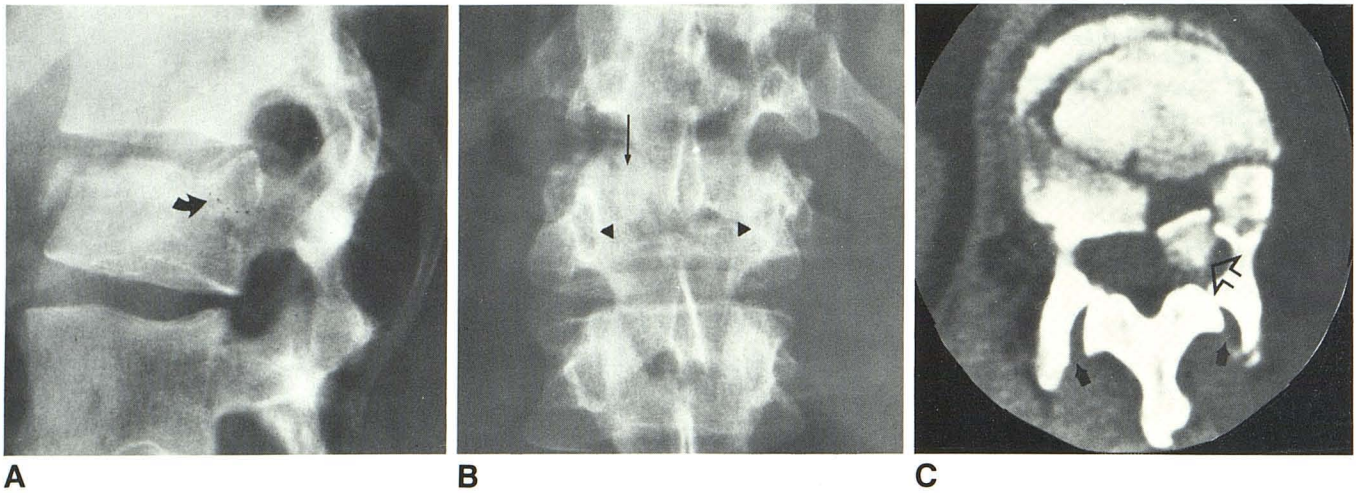
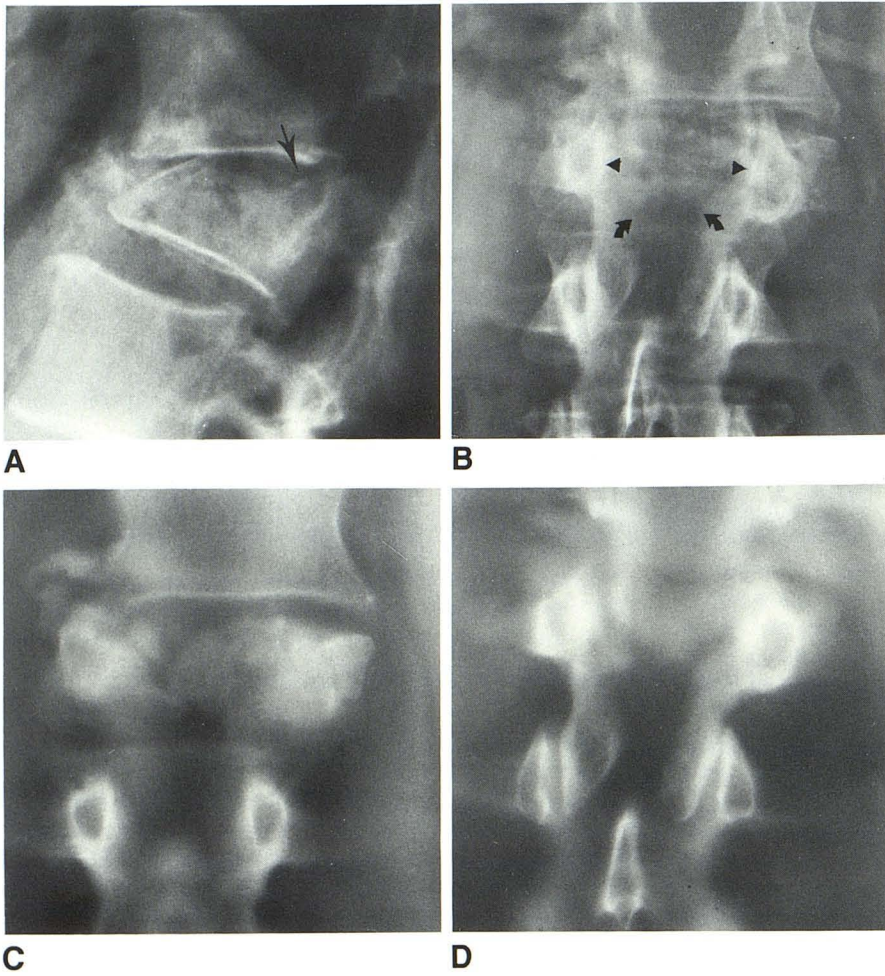Fig. 7.—Case 2. Unilateral burst (see text for full description). **A**, Lateral; **B**, Anteroposterior; **C**, Axial CT.

Fig. 8.—Case 3. Burst lateral translation (see text for full description). **A**, Lateral; **B**, Anteroposterior; **C**, Coronal tomogram; **D**, Coronal tomogram.

canal narrowing, the characteristic laminar fracture abutting the spinous process (curved arrow), and the sagittal vertebral body fracture (open arrow). The left facet joint is minimally widened (small arrows).

Case 2 Unilateral Burst (see Fig. 7). On the lateral view (Fig. 7A), the fragment can be easily identified emanating from the posterosuperior margin (arrow). Note the distortion of the superior margin of the vertebral body. On the anteroposterior

Fig. 9.—Case 4. Burst sagittal translation (see text for full description). **A**, Lateral; **B**, Anteroposterior; **C**, Lateral tomogram; **D**, Lateral tomogram.
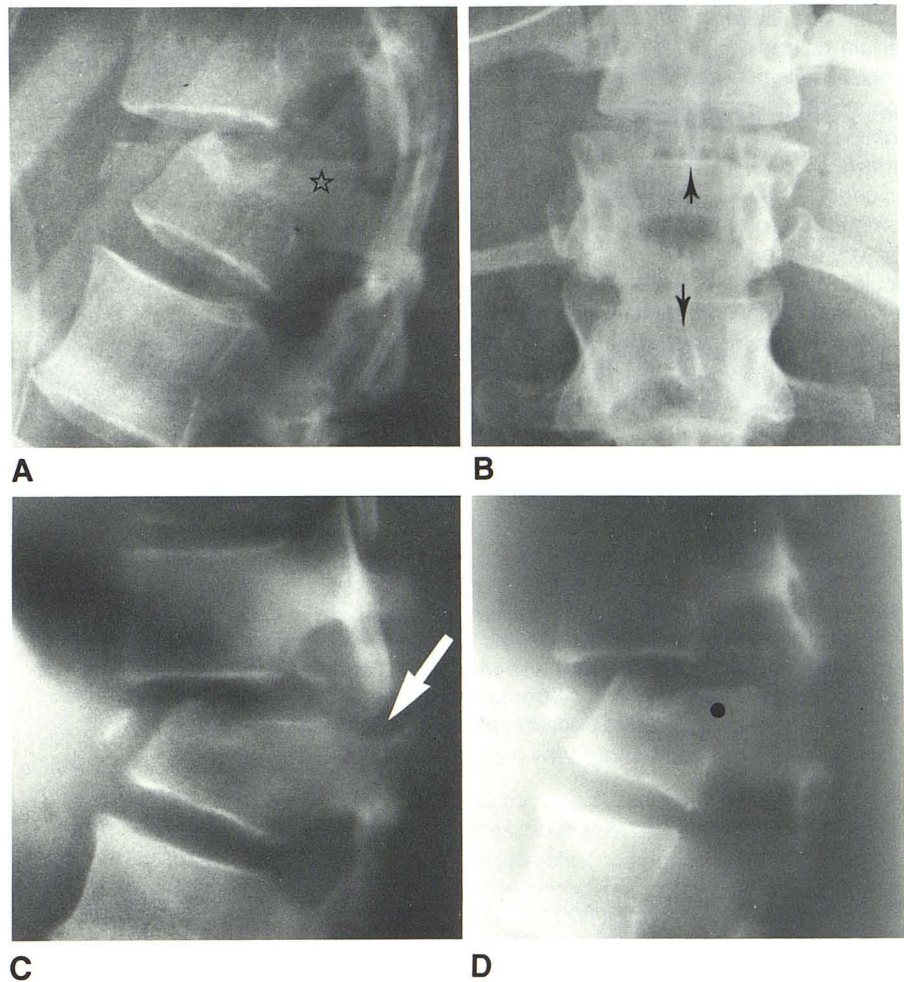
view (Fig. 7B), there is asymmetric lateral wedge deformity of the vertebral body, worse on the right (arrow). The interpediculate distance (IPD) is widened (arrowheads). The axial CT (Fig. 7C) demonstrates the unilateral burst fracture with the retropulsed fragment filling the left half of the spinal canal (open arrow). Note that the fragment has "flipped," so that its cortices face anteriorly. There is also bilateral facet subluxation (small arrows).

Case 3 Burst-Lateral Translation (see Fig. 8). The lateral view (Fig. 8A) demonstrates the burst fracture of L1, with typical fragment (arrow). Note the significant degree of kyphosis. The anteroposterior view (Fig. 8B) shows obvious lateral translation of the lumbar spine toward the left, widened IPD (arrowheads), and bilateral laminar fractures (curved arrows). Coronal tomography (Figs. 8C and 8D) demonstrates the vertical fracture components and marked lateral translation in this patient with incomplete neurologic deficit.

Case 4 Burst-Sagittal Translation (see Fig. 9). The lateral view (Fig. 9A) demonstrates wedge deformity of T12 with accompanying marked kyphosis. The retropulsed fragment is readily seen (star). On the anteorposterior view (Fig. 9B), note only minimal lateral translation. In this case, the IPD is not significantly widened when compared with that of the adjacent vertebral bodies. The interspinous distance (arrows) is in-

creased, indicating posterior element disruption. Lateral tomography (Figs. 9C and 9D) clearly identifies the unilateral facet lock (arrow) and the large retropulsed fragment (dot).

Discussion

Since its initial conceptualization by Holdsworth in 1963 [13], the burst fracture has been the subject of numerous radiologic, orthopedic, and neurosurgical investigations. These complex fractures result from an axial compressive load applied to the spinal column, with varying degrees of accompanying flexion and/or rotation. Characteristic components of the injury include: centripetally oriented disruption of the vertebral body, vertical fracture of the vertebra emanating from the basivertebral foramen, unilateral or bilateral posterior element fractures that abut the spinous process, marked anterior wedge deformity, increased interpediculate distance, and significant spinal canal narrowing by retropulsed fragment(s) from the posterosuperior (and posteroinferior) corners of the vertebra. Nearly all bursts occur from T9 to L5; double bursts, with or without contiguity, are found in less than 10% of cases. Associated neurologic deficit is the rule; it nearly always corresponds to the level of the burst rather than to the frequently found noncontiguous associated spine fracture.

With the advent and refinement of high-resolution CT, certain characteristic patterns can be delineated that allow precise definition and classification of the injury, aid in preoperative treatment planning, and help explain the frequently observed "unstable" nature of these uncommon spinal fractures [2, 3, 5, 8, 11, 14]. Radiographic indicators of instability include (1) the presence of translational components, (2) compression greater than 50% of vertebral body height, (3) fracture of the posterior elements, and (4) increased interpediculate distance. In our series, no definite prognostic difference could be discerned among the types of bursts and their associated retropulsed fragments. However, recognition of burst variants with their accompanying translations, and precise delineation of fragment anatomy, does aid in treatment planning.

While CT displays the components of the burst fracture and its fragments in unrivaled detail, and images can be obtained without significant patient manipulation, its use is not without pitfalls. Since axial imaging does not allow easy recognition of translational components, reformatting is necessary. In addition, more than half of associated vertebral body/posterior element fractures were not contiguous with the burst, and over 40% were found *more than two* levels from the burst. We recommend both lateral and anteroposterior views of the thoracic and lumbar spine in the emergency room as a routine. Plain tomography may be of value in some cases.

REFERENCES

1. Whitesides TE. Traumatic kyphosis of the thoracolumbar spine. *Clin Orthop* **1977**;128:78–92

2. McAfee PC, Yuan HA, Lasda NA. The unstable burst fracture. *Spine* **1982**;7:365–373
3. Jelsma RK, Kirsch PT, Rice JF, Jelsma LF. The radiographic description of thoracolumbar fractures. *Surg Neurol* **1982**;18:230–236
4. Malcom BW, Bradford DS, Winter RN, Chou SN. Post-traumatic kyphosis. A review of forty-eight surgically treated patients. *J Bone Joint Surg [Am]* **1981**;63A:891–899
5. Brant-Zawadzki M, Jeffrey RB, Minagi H, Pitts LH. High resolution CT of thoracolumbar fractures. *AJR* **1982**;138:699–704
6. Ferguson RL, Allen BL. A mechanistic classification of thoracolumbar spine fractures. *Clin Orthop* **1984**;189:77–88
7. Denis F, Armstrong GWD, Searls K, Matta L. Acute thoracolumbar burst fractures in the absence of neurologic deficit. *Clin Orthop* **1984**;189:142–149
8. Kilcoyne RF, Mack LA, King HA, Ratcliffe SS, Loop JW. Thoracolumbar spine injuries associated with vertical plunges: Reappraisal with computed tomography. *Radiology* **1983**;146:137–140
9. Hinck V, Clarke W, Hopkins C. Normal interpediculate distances (minimum and maximum) in children and adults. *AJR* **1966**;97:141–153
10. Holdsworth F. Fractures, dislocations and fracture-dislocations of the spine. *J Bone Joint Surg [Am]* **1970**;52A:1534–1551
11. Denis F. The three column spine and its significance in the classification of acute thoracolumbar spinal injuries. *Spine* **1983**;8:817–831
12. Smith GR, Northrop CH, Loop JW. Jumpers fractures: Patterns of thoracolumbar spine injuries associated with vertical plunges. *Radiology* **1977**;122:657–663
13. Holdsworth F. Fractures, dislocations and fracture-dislocations of the spine. *J Bone Joint Surg [BR]* **1963**;45B:6–20
14. Guerra J, Garfin SR, Resnick D. Vertebral burst fractures: CT analysis of the retropulsed fragment. *Radiology* **1984**;153:769–772